THE JOURNAL OF PHYSICAL CHEMISTRY Letters

Letter

Cite This: J. Phys. Chem. Lett. 2017, 8, 6226−6230

pubs.acs.org/JPCL

Insights into Solid-Electrolyte Interphase Induced Li-Ion Degradation from in Situ Auger Electron Spectroscopy

Ching-Yen Tang,[†] Yonghui Ma,[‡] Richard T. Haasch,[§] Jia-Hu Ouyang,[‡] and Shen J. Dillon*[,†,§]

[†]Department of Materials Science and Engineering, University of Illinois Urbana−Champaign, Urbana, Illinois 61801, United States

[‡]School of Materials Science and Engineering, Harbin Institute of Technology, Harbin 150001, China

[§]Materials Research Laboratory, University of Illinois Urbana−Champaign, Urbana, Illinois 61801, United States

Supporting Information

ABSTRACT: Surface reactions occurring on $LiMn_2O_4$, $LiCoO_2$, $LiNiO_2$, $Li[Ni_{1/3}Mn_{1/3}Co_{1/3}]O_2$, and $LiFePO_4$ during charging and overcharging are studied by in situ and ex situ Auger electron spectroscopy. Carbon surface stability at the cathode solid-electrolyte interphase (SEI), associated with carbonate formation, decomposition, and CO/CO_2 evolution, on different electrodes during cycling correlates with their cycle life. To understand how associated CO and CO_2 evolution affects cycle stability, $LiMn_2O_4$ is cycled in flowing gas. Flowing Ar enhances cycle life by a factor of 2, while flowing Ar with 1% CO_2 reduces cycle life by a factor of 2. CO_2 is proposed to degrade cycle life by trapping Li and metal ions as carbonate in the anode SEI.

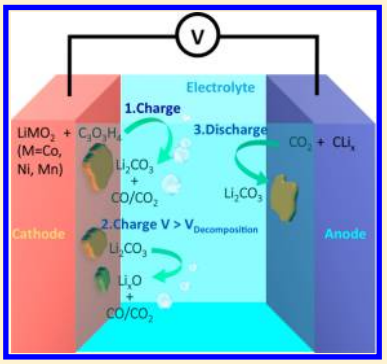

Processes limiting secondary battery cycle life elicit great interest, because capacity fade constrains the lifetime costs of energy storage systems. Elucidating mechanisms for capacity fade remains an ongoing challenge owing to the large phase space of battery chemistries and cycling conditions; difficulty in analytically and structurally characterizing system evolution at all appropriate length scales over many cycles; and the complex nature of relevant interactions between mechanical, chemical, structural, and electrical processes.[1,2] Li-ion battery cycle life is sensitive to cathode chemistry, but half-cell experiments reveal that they do not degrade nearly as rapidly as full cells.[3,4] Similarly, carbon-based anodes exhibit much better cycle stability in half cells than full cells.[3,5] Capacity fade in many systems arises from the loss of redox active material (e.g., Li) in unwanted, so-called "side reactions". Capacity fade sensitivity to cathode chemistry suggests they play an important role in instigating side reactions that cause capacity fade. However, the reactions that directly result in capacity loss may be spatially delocalized from the cathode. One well-known example occurs in Mn-containing cathodes, such as $LiMn_2O_4$ (LMO) and related compounds.[6−13] While some of the detailed mechanisms are still the subject of debate, it is known that during cycling Mn(II) dissolves from the LMO surface and is subsequently deposited on the anode's solid electrolyte interphase (SEI), which is thought to be primarily an electrolyte decomposition product on the anode.[14−17] The Mn is said to increase the impedance of what would otherwise be an electrochemically more favorable SEI. This can lead to a loss of accessible Li and degrade the overall capacity of the cell. Mn(II) dissolution is sensitive to a number of factors such as potential, electrode chemistry, and in particular H^+ impurities in the electrolyte, often believed to originate from H_2O impurities absorbed during processing.[8,14,18] Proposed electrolyte degradation reactions have also been associated with H^+ production (i.e., deprotonation of molecules such as $C_3H_4O_3$).[19] Thus, the increase in anode SEI impedance believed to be critical in capacity fade is linked to a spatially distinct cathode Mn(II) dissolution mechanism, which in turn may be sensitive to electrolyte decomposition reactions occurring elsewhere on the anode and/or cathode.[14,15] Recent experiments characterizing gas evolved from full cells versus half cells indicate interactions between species evolved at the opposing electrodes.[20,21] Thus, we anticipate that such reactions could be similarly important in affecting cycle life, while also being sensitive to electrode chemistry.

To investigate surface reactions that could induce capacity fade, we recently developed in situ Auger electron spectroscopy (AES) and in situ X-ray photoelectron spectroscopy (XPS) to characterize the evolution of surface chemistry and bonding in model ultrahigh vacuum environments (UHV; here $\approx 10^{-6}$ Pa). The approach places electrode particles on an ≈30 nm amorphous C membrane that serves as both a current collector and a Li permeable membrane that isolates adjacent ionic liquid electrolyte. Prior work on LMO established that the technique is quite reproducible and that surface composition measured in situ closely mimics surface composition measured ex situ from samples cycled in commercial electrolyte. Specifically, Li_2CO_3 dominated the surface reaction products in both cases and was

Received: October 26, 2017
Accepted: December 12, 2017
Published: December 12, 2017

DOI: 10.1021/acs.jpclett.7b02847
J. Phys. Chem. Lett. 2017, 8, 6226−6230

present at similar concentrations in situ and ex situ at each applied potential. The UHV contains CO, CO_2, organic contaminants, and ionic liquid vapor as sources for C oxidation during the in situ experiments, while ethylene carbonate (EC) and dimethyl carbonate (DMC) serve as primary sources in our electrolyte for the ex situ experiments. Soaking in EC−DMC, and related electrolytes, is known to induce Li_2CO_3 formation on some oxide electrodes and has often been attributed to bonding of the organic's carbonate group to the cathode.[22] However, half-cell gas evolution experiments indicate that CO and CO_2 primarily evolve from the cathode with few alkyl groups observed.[23] Our model in situ experiments agree, suggesting that oxide cathodes favor oxidation of the alkyl group, or in our case organic contaminants and CO in the UHV. The second notable observation from this work was that the surface Li_2CO_3 decomposed between 4.05 and 4.2 V. The Li_2CO_3 formation and decomposition reactions occur within the typical cycling window of LMO and each process is anticipated to evolve CO and/or CO_2. Half-cell experiments have been performed to investigate CO_2 reactions with electrodes. Graphite-based half cells were relatively unaffected by the presence of CO_2, while $LiCoO_2$ half cells exhibited improved cycle stability, presumably due to CO_2 stabilizing the Li metal anode SEI.[24,25] Recently published work shows that dosing a $LiCoO_2$−Si full cell with solid CO_2 extends cycle life by enabling the Si to develop a more favorable SEI.[26] In this work, we compare C redox and Li_2CO_3 stability on the surfaces of different oxides using in situ AES and correlate this with cycle life. We further investigate the relative importance of CO and CO_2 in affecting full cell cycle life by flowing mixed gases across an ex situ cell during cycling.

Figure 1 shows the evolution of surface chemistry of $LiMn_2O_4$ (LMO), $LiCoO_2$ (LCO), $LiNiO_2$ (LNO), $Li[Ni_{1/3}Mn_{1/3}Co_{1/3}]O_2$ (NMC), and $LiFePO_4$ (LFP) during charging and overcharging conditions. The C-to-cation ratio is used here as a reasonable proxy for changes in surface C concentration. LMO and LNO exhibit similar behavior where C concentration increases then decreases as voltage increases. The AES peaks provide qualitative bonding information through fingerprinting (see Figure S1). Carbon on both LMO and LNO exhibits carbonate character below 4.6 V. However, reduction in C concentration occurs by decomposition of some of the Li_2CO_3, forming gas (e.g., CO or CO_2). LCO and LFP exhibit relatively more stable C concentrations (≈25−30%) with increasing potential. LFP never displays Li_2CO_3 like bonding consistent with its tendency to form graphitic surface carbons during synthesis.[27] LCO shows less Li_2CO_3 like bonding above 4.4 V despite its C concentration being more stable. This suggests CO_2 does not evolve as readily from Li_2CO_3 decomposition on LCO. Similarly, LFP should evolve less CO/CO_2 then LNO and LMO in their typical cycling windows. NMC maintains a relatively low C concentration at all voltages below ≈4.7 V, indicating limited C oxidation and relative surface stability, which in this range will lead to limited CO/CO_2 evolution. At 4.7 and 4.8 V, high concentrations of C, bonded like Li_2CO_3, are observed. Time-dependent measurements indicate that the C concentration decays with time at open-circuit voltage (OCV) at these potentials, where O loss from the lattice is well-known (see Figure S2). While it is somewhat outside the scope of this Letter, the results suggest the mechanism for O loss is C oxidation on the surface to form Li_2CO_3 and its subsequent decomposition to CO/CO_2. This reaction sequence is likely kinetically favorable, given the thermodynamic instability of bulk Li_2CO_3 at these potentials.[28]

We note that ex situ AES measurements of the surface chemistry of LCO, LNO, and LMO samples equilibrated at the same potentials mostly agree with the in situ experiments (see Figure S3). The most significant differences relate to the C concentration measured in the "pristine state", where the ex situ electrodes were initially processed in NMP, which can leave residual C. The combination of in situ and ex situ experiments leads us to hypothesize that increases in C concentration in EC, for example, should occur by either

$$\mathrm{Li}_y\mathrm{MO}_2 \Leftrightarrow x\mathrm{Li}_2\mathrm{O} + \mathrm{Li}_{y-2x}\mathrm{MO}_{2-x} \quad (\mathrm{M} = \mathrm{Co, Ni, Mn})$$
$$\mathrm{C}_3\mathrm{H}_4\mathrm{O}_3 + 2\mathrm{Li}_2\mathrm{O} \Leftrightarrow 2\mathrm{Li}_2\mathrm{CO}_3 + \mathrm{CO} + 4\mathrm{H}^+ + 4\mathrm{e}^- \quad (1)$$

or

$$\mathrm{Li}_y\mathrm{MO}_2 \Leftrightarrow x\mathrm{Li}_2\mathrm{O}_2 + \mathrm{Li}_{y-2x}\mathrm{MO}_{2-2x} \quad (\mathrm{M} = \mathrm{Co, Ni, Mn})$$
$$\mathrm{C}_3\mathrm{H}_4\mathrm{O}_3 + 2\mathrm{Li}_2\mathrm{O}_2 \Leftrightarrow 2\mathrm{Li}_2\mathrm{CO}_3 + \mathrm{CO}_2 + 4\mathrm{H}^+ + 4\mathrm{e}^- \quad (2)$$

The electrons produced in the reaction will reduce the M cations locally at the surface. Decreases in C surface concentration could occur by either

$$\mathrm{Li}_2\mathrm{CO}_3 \Leftrightarrow \mathrm{Li}_2\mathrm{O}_x + \mathrm{CO}_{3-x} \quad (3)$$

or a related CO/CO_2 evolving reaction involving charge transfer with the cathode. In terms of C stability NMC > LFP > LCO > LNO > LMO, and the same trend holds for cycle life (NMC > LFP > LCO > LNO > LMO). In fact, there is a clear trend between 30 cycle capacity fade reported for these materials and a carbon instability metric $\Theta = \sum_{i=V_{OCV}}^{V_{max}} \left|\Delta\frac{\%C}{\%M}\right| \Delta V_i$ which integrates the absolute value of change in C/M concentration over the voltage window of

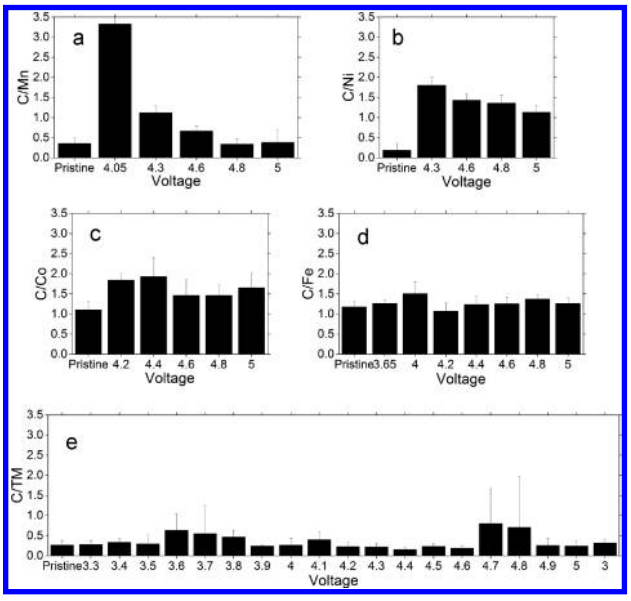

Figure 1. C concentration versus V for different cathodes during in situ charging and overcharging in the AES: (a) LMO [The data is the average of two sets of experiments, one with TFSI electrolyte (4.3, 4.6, 4.8, and 5 V) and one from BF_4 electrolyte (4.05, 4.3, and 4.6 V).], (b) LNO, (c) LCO, (d) LFP, and (e) NMC (TM, transition metal).

DOI: 10.1021/acs.jpclett.7b02847
J. Phys. Chem. Lett. 2017, 8, 6226−6230

interest as shown in Figure 2. We therefore hypothesize that either CO or CO_2 should affect full cell cycle life, possibly

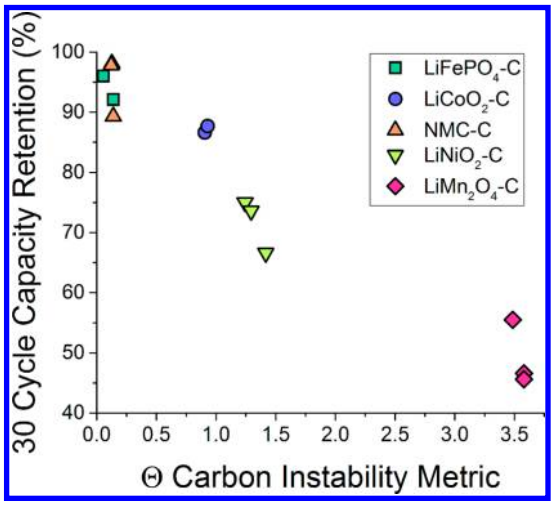

Figure 2. Reported[34−43] 30 cycle capacity retention values plotted against $\Theta = \sum_{i=V_{OCV}}^{V_{max}} \left|\Delta\frac{\%C}{\%M}\right| \Delta V_i$, a carbon instability metric that integrates the absolute value of change in C/M concentration over the voltage window of interest. Note that linear interpolation was utilized when the upper bound of the voltage window occurred between two measured values. Table S1 includes more details about the reported cycling experiments. As carbon instability increases in the cycling window of a particular electrode material, the capacity retention diminishes.

through its subsequent reduction on the anode during charging or reduction on the cathode during discharging.

We assembled 4-way Swagelok cells (see Figure S4) and compared the capacity fade behavior of LMO electrodes cycled as full cells against graphite between 3.0 and 4.3 V with different gas chemistries flowing at a rate of 20 cc/min and a pressure of 25 psi (see Figure 3). We compare the cycle life of a

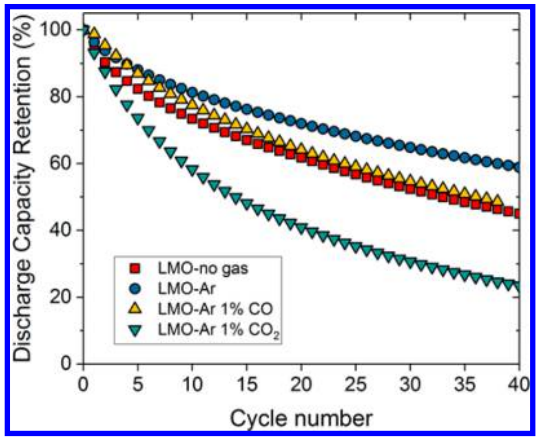

Figure 3. Effect of flowing gas chemistry on $LiMn_2O_4$−C full cell cycle life.

static battery with those under flowing Ar, Ar−1% CO, and Ar−1% CO_2. We note that the compositions are somewhat arbitrary, as the solution thermodynamics between CO, CO_2, and the electrolyte are unknown. A pristine cell will have almost no CO/CO_2 present, while a well-aged cell may have high concentrations of CO/CO_2 present. Here we only seek to demonstrate the feasibility of CO_2 strongly participating in capacity fade. The flow of Ar improves cycle life by ≈2×, possibly by "flushing" unwanted gas product from the cell. Ar−1% CO produces similar cycle life as the static cell. Most noticeably, Ar−1% CO_2 leads to rapid capacity fade. A factor of ≈4 difference in rate of fade is observed between the cell with pure Ar versus Ar−1% CO_2. The cell cycled in Ar exhibited negligible impedance growth, while cycling in Ar−1% CO_2 promoted significant impedance growth (see Figure S5). These data support our hypothesis that CO_2-evolving surface reactions occurring on the cathode influence full cell cycle life. CO_2 likely reacts with reduced Li intercalated in graphite through the highly exothermic chemical reaction

$$2Li + 2CO_2 \Leftrightarrow Li_2CO_3 + CO \quad (4)$$

as well as direct electrochemical reduction

$$CO_2 + 4e^- \Leftrightarrow C + 2O_2 \quad (5)$$

and related reactions. This is supported by ex situ AES results measured from samples soaked in electrolyte, cycled under static conditions, cycled in flowing Ar, and in flowing Ar−1% CO_2. We found it informative to observe the back surface of the Cu current collector to avoid measuring C from the active anode, binder and conductive C. Cycling in CO_2 produces a C-rich surface (61.2%) on the Cu (Figure 4). Samples cycled in

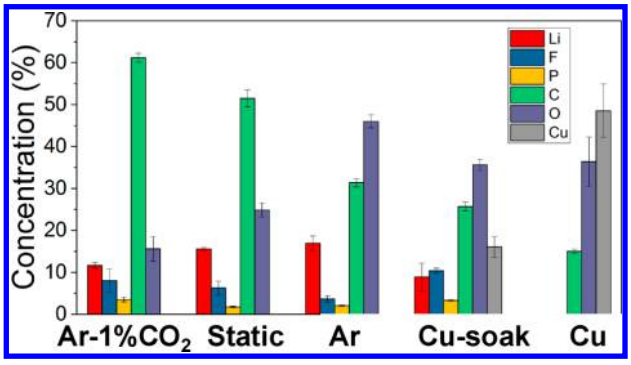

Figure 4. Surface composition measured by ex situ AES from the back sides of Cu current collectors after 5 cycles in a flowing Ar−1% CO_2, flowing Ar, or static cell. The Cu current collector soaked in electrolyte and the bare Cu current collector are included for comparison.

Ar have more O rich surfaces (46.0%), with about half the C concentration (31.4%) of the samples cycled in Ar−1% CO_2. The surface chemistry of the static cells is intermediate to these samples. XPS reveals similar trends in bulk composition (Figure S6). Analysis of the C and O XPS peaks, shown in Figure 5, indicate that samples cycled in Ar have more carbonyl and Li_2O groups and less carbonate groups than the samples cycled in Ar−1% CO_2. We cannot discount the possibility of catalytic effects associated with SEI formation on graphite versus the Cu model utilized here. For example, we anticipate the carbonate formation reaction will be exacerbated by the higher Li chemical potential at the active anode particles. The accumulation of CO_3^{2-} in cells containing CO_2 is consistent with the anticipated chemical and electrochemical CO_2 reduction pathways in reaction 4. Reaction 4 will directly degrade capacity because bulk Li_2CO_3 is stable within the voltage window of C anodes; thus, its formation will permanently remove active Li from the system.[21] A competing reaction could also be CO_2 reduction coupled with metal ion reactions to form metal carbonates on the anode, such as $MnCO_2$ when cycling LMO. Gas evolution experiments

DOI: 10.1021/acs.jpclett.7b02847
J. Phys. Chem. Lett. 2017, 8, 6226−6230

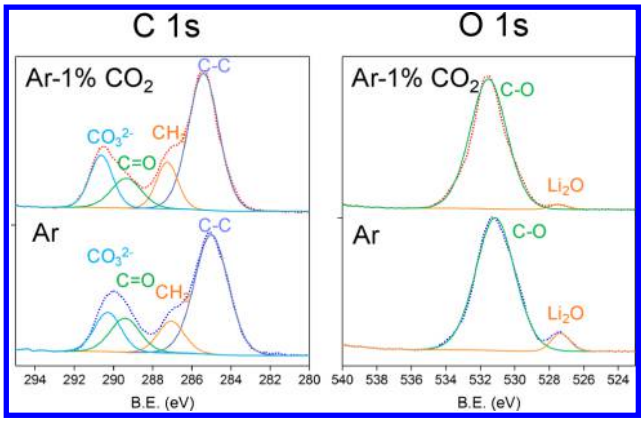

Figure 5. XPS scans of the reverse side of the Cu current collector after 5 cycles in flowing Ar and Ar−1% CO_2. A table summarizing the relative compositions can be found in the Supporting Information.

indicate that CO_2 evolves each cycle, consistent with our observations in LMO that the instability in surface C is observed beyond the first cycle.[21] Therefore, a CO_2-based mechanism for capacity fade could persist over many cycles in systems like LMO.

CO_2 has limited effect on graphite anode half cell capacity, as reported in ref 24, suggesting that the Li trapping reaction does not significantly affect electrode impedance. CO_2 improves $LiCoO_2$ half cell cycle life.[25] In ref 25 this was attributed to the formation of a more favorable SEI on Li metal through CO_2 reduction. In both cases, trapping Li in a stable Li_2CO_3 will not affect half-cell cycle life, because the Li capacity of the metallic anode far exceeds the counter electrode capacity. Recent experiments dosing $LiCoO_2$−Si full cells with discrete amounts of CO_2 demonstrated improved cycle life due to the presence of the CO_2, which also favors the formation of stable SEI.[26] Despite its beneficial role in promoting SEI stability, persistent CO_2 generation will ultimately lead to Li loss from the system and capacity fade. Because CO_2 induces capacity fade, we anticipate additives and chemistries that suppress or getter CO_2 should improve cycle life. For example, vinylene carbonate suppresses CO_2 evolution at room temperature and is also correlated with improving cycle life.[29] H_2O and H^+ impurities have been shown to destabilize Li_2CO_3 on the cathode and also degrade cycle life in most systems.[30] A range of approaches have been investigated for CO_2 capture, including reactions with alkaline metals, absorption by metal−organic frameworks and related structures, reactions with amines, etc.[31−33]

We observed that C surface instability on cathodes during cycling correlates with measured full cell cycle life. Because the C instability must be associated with CO and/or CO_2 evolution, we tested the effects of these gases on cycle life and found CO_2 degrades LMO-C full cells. We hypothesize that the presence of CO_2 causes Li and/or Mn to become trapped in the anode SEI, leading to the loss of the electroactive species and increased impedance. This hypothesis was supported by ex situ AES and XPS characterization of SEI on the Cu current collector. However, we note that future studies will need to be carried out in order to (i) isolate the effects of evolved gas and protons on the anode versus cathode and (ii) definitively identify the specific reactions dominating the capacity fade.

■ ASSOCIATED CONTENT

Supporting Information

The Supporting Information is available free of charge on the ACS Publications website at DOI: 10.1021/acs.jpclett.7b02847.

Additional experimental details, figures, and tables (PDF)

■ AUTHOR INFORMATION

Corresponding Author

*E-mail: sdillon@illinois.edu.

ORCID

Ching-Yen Tang: 0000-0002-8003-6825
Richard T. Haasch: 0000-0001-9479-2595
Shen J. Dillon: 0000-0002-6192-4026

Notes

The authors declare no competing financial interest.

■ ACKNOWLEDGMENTS

S.J.D. and C.-Y.T. acknowledge support from National Science Foundation under Grant No. 1254406. Y.M. gratefully acknowledges the financial support from China Scholarship Council. We also acknowledge Dr. J. Nanda for providing NMC material for testing and discussion. This work was carried out in part at the Materials Research Laboratory Central Research Facilities, University of Illinois.

■ REFERENCES

(1) Hausbrand, R.; Cherkashinin, G.; Ehrenberg, H.; Gröting, M.; Albe, K.; Hess, C.; Jaegermann, W. Fundamental degradation mechanisms of layered oxide Li-ion battery cathode materials: Methodology, insights and novel approaches. *Mater. Sci. Eng., B* **2015**, *192*, 3−25.

(2) Jung, S.-K.; Gwon, H.; Hong, J.; Park, K.-Y.; Seo, D.-H.; Kim, H.; Hyun, J.; Yang, W.; Kang, K. Understanding the Degradation Mechanisms of $LiNi_{0.5}Co_{0.2}Mn_{0.3}O_2$ Cathode Material in Lithium Ion Batteries. *Adv. Energy Mater.* **2014**, *4* (1), 1300787.

(3) Kim, J.-H.; Pieczonka, N. P. W.; Li, Z.; Wu, Y.; Harris, S.; Powell, B. R. Understanding the capacity fading mechanism in $LiNi_{0.5}Mn_{1.5}O_4$/graphite Li-ion batteries. *Electrochim. Acta* **2013**, *90*, 556−562.

(4) Ziv, B.; Borgel, V.; Aurbach, D.; Kim, J.-H.; Xiao, X.; Powell, B. R. Investigation of the Reasons for Capacity Fading in Li-Ion Battery Cells. *J. Electrochem. Soc.* **2014**, *161* (10), A1672−A1680.

(5) Yao, X. L.; Xie, S.; Chen, C. H.; Wang, Q. S.; Sun, J. H.; Li, Y. L.; Lu, S. X. Comparisons of graphite and spinel $Li_{1.33}Ti_{1.67}O_4$ as anode materials for rechargeable lithium-ion batteries. *Electrochim. Acta* **2005**, *50* (20), 4076−4081.

(6) Aurbach, D.; Gamolsky, K.; Markovsky, B.; Gofer, Y.; Schmidt, M.; Heider, U. On the use of vinylene carbonate (VC) as an additive to electrolyte solutions for Li-ion batteries. *Electrochim. Acta* **2002**, *47* (9), 1423−1439.

(7) Aurbach, D.; Markovsky, B.; Salitra, G.; Markevich, E.; Talyossef, Y.; Koltypin, M.; Nazar, L.; Ellis, B.; Kovacheva, D. Review on electrode−electrolyte solution interactions, related to cathode materials for Li-ion batteries. *J. Power Sources* **2007**, *165* (2), 491−499.

(8) Jang, D. H.; Shin, Y. J.; Oh, S. M. Dissolution of Spinel Oxides and Capacity Losses in 4 V $Li/Li_xMn_2O_4$ Cells. *J. Electrochem. Soc.* **1996**, *143* (7), 2204−2211.

(9) Tarascon, J. M.; McKinnon, W. R.; Coowar, F.; Bowmer, T. N.; Amatucci, G.; Guyomard, D. Synthesis Conditions and Oxygen Stoichiometry Effects on Li Insertion into the Spinel $LiMn_2O_4$. *J. Electrochem. Soc.* **1994**, *141* (6), 1421−1431.

(10) Tarascon, J. M.; Wang, E.; Shokoohi, F. K.; McKinnon, W. R.; Colson, S. The Spinel Phase of $LiMn_2O_4$ as a Cathode in Secondary Lithium Cells. *J. Electrochem. Soc.* **1991**, *138* (10), 2859−2864.

DOI: 10.1021/acs.jpclett.7b02847
J. Phys. Chem. Lett. 2017, 8, 6226−6230

(11) Thackeray, M. M.; Johnson, P. J.; de Picciotto, L. A.; Bruce, P. G.; Goodenough, J. B. Electrochemical extraction of lithium from $LiMn_2O_4$. *Mater. Res. Bull.* **1984**, *19* (2), 179−187.
(12) Xia, Y.; Yoshio, M. An Investigation of Lithium Ion Insertion into Spinel Structure Li-Mn-O Compounds. *J. Electrochem. Soc.* **1996**, *143* (3), 825−833.
(13) Xia, Y.; Zhou, Y.; Yoshio, M. Capacity Fading on Cycling of 4 V $Li/LiMn_2O_4$ Cells. *J. Electrochem. Soc.* **1997**, *144* (8), 2593−2600.
(14) Appiah, W. A.; Park, J.; Byun, S.; Ryou, M.-H.; Lee, Y. M. A Mathematical Model for Cyclic Aging of Spinel $LiMn_2O_4$/Graphite Lithium-Ion Cells. *J. Electrochem. Soc.* **2016**, *163* (13), A2757−A2767.
(15) Kim, D.; Park, S.; Chae, O. B.; Ryu, J. H.; Kim, Y.-U.; Yin, R.-Z.; Oh, S. M. Re-Deposition of Manganese Species on Spinel $LiMn_2O_4$ Electrode after Mn Dissolution. *J. Electrochem. Soc.* **2012**, *159* (3), A193−A197.
(16) Manthiram, A.; Chemelewski, K.; Lee, E.-S. A perspective on the high-voltage $LiMn_{1.5}Ni_{0.5}O_4$ spinel cathode for lithium-ion batteries. *Energy Environ. Sci.* **2014**, *7* (4), 1339−1350.
(17) Tsunekawa, H.; Tanimoto, S.; Marubayashi, R.; Fujita, M.; Kifune, K.; Sano, M. Capacity Fading of Graphite Electrodes Due to the Deposition of Manganese Ions on Them in Li-Ion Batteries. *J. Electrochem. Soc.* **2002**, *149* (10), A1326−A1331.
(18) Chen, J. S.; Wang, L. F.; Fang, B. J.; Lee, S. Y.; Guo, R. Z. Rotating ring-disk electrode measurements on Mn dissolution and capacity losses of spinel electrodes in various organic electrolytes. *J. Power Sources* **2006**, *157* (1), 515−521.
(19) Leung, K. First-Principles Modeling of Mn(II) Migration above and Dissolution from $LixMn_2O_4$ (001) Surfaces. *Chem. Mater.* **2017**, *29* (6), 2550−2562.
(20) Xiong, D. J.; Petibon, R.; Nie, M.; Ma, L.; Xia, J.; Dahn, J. R. Interactions between Positive and Negative Electrodes in Li-Ion Cells Operated at High Temperature and High Voltage. *J. Electrochem. Soc.* **2016**, *163* (3), A546−A551.
(21) Metzger, M.; Strehle, B.; Solchenbach, S.; Gasteiger, H. A. Origin of H_2 Evolution in LIBs: H_2O Reduction vs. Electrolyte Oxidation. *J. Electrochem. Soc.* **2016**, *163* (5), A798−A809.
(22) Aurbach, D.; Gamolsky, K.; Markovsky, B.; Salitra, G.; Gofer, Y.; Heider, U.; Oesten, R.; Schmidt, M. The Study of Surface Phenomena Related to Electrochemical Lithium Intercalation into Li x MO y Host Materials (M = Ni, Mn). *J. Electrochem. Soc.* **2000**, *147* (4), 1322−1331.
(23) Castel, E.; Berg, E. J.; El Kazzi, M.; Novák, P.; Villevieille, C. Differential Electrochemical Mass Spectrometry Study of the Interface of $xLi_2MnO_3\cdot(1-x)LiMO_2$ (M = Ni, Co, and Mn) Material as a Positive Electrode in Li-Ion Batteries. *Chem. Mater.* **2014**, *26* (17), 5051−5057.
(24) Levi, M. D.; Markevich, E.; Wang, C.; Koltypin, M.; Aurbach, D. The effect of dimethyl pyrocarbonate on electroanalytical behavior and cycling of graphite electrodes. *J. Electrochem. Soc.* **2004**, *151* (6), A848−A856.
(25) Plichta, E.; Slane, S.; Uchiyama, M.; Salomon, M.; Chua, D.; Ebner, W. B.; Lin, H. W. An Improved Li/Li_xCoO_2 Rechargeable Cell. *J. Electrochem. Soc.* **1989**, *136* (7), 1865−1869.
(26) Krause, L. J.; Chevrier, V. L.; Jensen, L. D.; Brandt, T. The Effect of Carbon Dioxide on the Cycle Life and Electrolyte Stability of Li-Ion Full Cells Containing Silicon Alloy. *J. Electrochem. Soc.* **2017**, *164* (12), A2527−A2533.
(27) Wang, Y.; Wang, Y.; Hosono, E.; Wang, K.; Zhou, H. The Design of a $LiFePO_4$/Carbon Nanocomposite With a Core−Shell Structure and Its Synthesis by an In Situ Polymerization Restriction Method. *Angew. Chem., Int. Ed.* **2008**, *47* (39), 7461−7465.
(28) Tang, C.-Y.; Leung, K.; Haasch, R. T.; Dillon, S. J. $LiMn_2O_4$ surface chemistry evolution during cycling revealed by in situ Auger Electron Spectroscopy and X-ray Photoelectron Spectroscopy. *ACS Appl. Mater. Interfaces* **2017**, *9*, 33968.
(29) Vetter, J.; Holzapfel, M.; Wuersig, A.; Scheifele, W.; Ufheil, J.; Novák, P. In situ study on CO_2 evolution at lithium-ion battery cathodes. *J. Power Sources* **2006**, *159* (1), 277−281.
(30) Bi, Y.; Wang, T.; Liu, M.; Du, R.; Yang, W.; Liu, Z.; Peng, Z.; Liu, Y.; Wang, D.; Sun, X. Stability of Li_2CO_3 in cathode of lithium ion battery and its influence on electrochemical performance. *RSC Adv.* **2016**, *6* (23), 19233−19237.
(31) Bhatta, L. K. G.; Subramanyam, S.; Chengala, M. D.; Olivera, S.; Venkatesh, K. Progress in hydrotalcite like compounds and metal-based oxides for CO_2 capture: a review. *J. Cleaner Prod.* **2015**, *103*, 171−196.
(32) Zheng, B.; Liu, H.; Wang, Z.; Yu, X.; Yi, P.; Bai, J. Porous NbO-type metal-organic framework with inserted acylamide groups exhibiting highly selective CO_2 capture. *CrystEngComm* **2013**, *15* (18), 3517−3520.
(33) Zelenak, V.; Halamova, D.; Gaberova, L.; Bloch, E.; Llewellyn, P. Amine-modified SBA-12 mesoporous silica for carbon dioxide capture: Effect of amine basicity on sorption properties. *Microporous Mesoporous Mater.* **2008**, *116* (1), 358−364.
(34) Sun, S.; Guan, T.; Leng, K.; Gao, Y.; Cheng, X.; Yin, G. Changes of Degradation Mechanisms of $LiFePO_4$/Graphite Batteries Cycled at Different Ambient Temperatures. *Electrochim. Acta* **2017**, *237*, 248−258.
(35) Shim, J.; Striebel, K. A. Cycling performance of low-cost lithium ion batteries with natural graphite and $LiFePO_4$. *J. Power Sources* **2003**, *119*, 955−958.
(36) Lee, J.-N.; Lee, J.-N.; Han, G.-B.; Ryou, M. H.; Lee, D. J.; Song, J.; Choi, H. W.; Park, J.-K. N-(triphenylphosphoranylidene) aniline as a novel electrolyte additive for high voltage $LiCoO_2$ operations in lithium ion batteries. *Electrochim. Acta* **2011**, *56*, 5195−5200.
(37) Kalluri, S.; Yoon, M.; Jo, M.; Park, S.; Myeong, S.; Kim, J.; Dou, S. X.; Guo, Z.; Cho, J. Surface Engineering Strategies of Layered $LiCoO_2$ Cathode Material to Realize High-Energy and High-Voltage Li-Ion Cells. *Adv. Energy Mater.* **2017**, *7*, 1601507.
(38) Jung, R.; Metzger, M.; Maglia, F.; Stinner, C.; Gasteiger, H. A. Oxygen Release and Its Effect on the Cycling Stability of $LiNi_xMn_yCo_zO_2$ (NMC) Cathode Materials for Li-Ion Batteries. *J. Electrochem. Soc.* **2017**, *164*, A1361−A1377.
(39) Dahn, J. R.; von Sacken, U.; Juzkow, M. W.; Al-Janaby, H. Rechargeable $LiNiO_2$/Carbon Cells. *J. Electrochem. Soc.* **1991**, *138*, 2207−2211.
(40) Tabuchi, M.; Kuriyama, N.; Takamori, K.; Imanari, Y.; Nakane, K. Appearance of Lithium-Excess $LiNiO_2$ with High Cyclability Synthesized by Thermal Decomposition Route from $LiNiO_2$-Li_2NiO_3 Solid Solution. *J. Electrochem. Soc.* **2016**, *163*, A2312−A2317.
(41) Moshtev, R. V.; Zlatilova, P.; Puresheva, B.; Manev, V. Material balance of petroleum coke/$LiNiO_2$ lithium-ion cells. *J. Power Sources* **1995**, *56*, 137−144.
(42) Wang, C.; Lu, S.; Kan, S.; Pang, J.; Jin, W.; Zhang, X. Enhanced capacity retention of Co and Li doubly doped $LiMn_2O_4$. *J. Power Sources* **2009**, *189*, 607−610.
(43) Yamagiwa, K.; Morita, D.; Yabuuchi, N.; Tanaka, T.; Fukunishi, M.; Taki, T.; Watanabe, H.; Otsuka, T.; Yano, T.; Son, J.-Y.; Cui, Y.-T.; Oji, H.; Komaba, S. Improved High-Temperature Performance and Surface Chemistry of Graphite/$LiMn_2O_4$ Li-Ion Cells by Fluorosilane-Based Electrolyte Additive. *Electrochim. Acta* **2015**, *160*, 347−356.

DOI: 10.1021/acs.jpclett.7b02847
J. Phys. Chem. Lett. 2017, 8, 6226−6230